Elasticity of post-perovskite $MgSiO_3$

Taku Tsuchiya, Jun Tsuchiya, Koichiro Umemoto, and Renata M. Wentzcovitch

Department of Chemical Engineering and Materials Science, Minnesota Supercomputing Institute for Digital Technology and Advanced Computation, University of Minnesota, Minneapolis, Minnesota, USA

Received 16 April 2004; revised 10 June 2004; accepted 16 June 2004; published 17 July 2004.

[1] We have determined by first principles the athermal elastic constant tensor, single crystal and aggregated acoustic velocities, and anisotropy of the recently discovered post-perovskite $MgSiO_3$ polymorph. This phase may be the most abundant mineral in the D″ region. We find that the post-perovskite phase has similar bulk modulus and larger shear modulus than perovskite at relevant pressures. This phase is remarkably anisotropic. Analyses of horizontal shear wave splittings in transversely isotropic aggregates indicate that diverse lattice preferred orientations could produce large variation in anisotropy consistent with seismic observations in D″. *INDEX TERMS:* 1025 Geochemistry: Composition of the mantle; 3909 Mineral Physics: Elasticity and anelasticity; 3924 Mineral Physics: High-pressure behavior; 5102 Physical Properties of Rocks: Acoustic properties; 7207 Seismology: Core and mantle. **Citation:** Tsuchiya, T., J. Tsuchiya, K. Umemoto, and R. M. Wentzcovitch (2004), Elasticity of post-perovskite $MgSiO_3$, *Geophys. Res. Lett.*, *31*, L14603, doi:10.1029/2004GL020278.

1. Introduction

[2] Very recently, a post-perovskite transition in $MgSiO_3$ was found by in situ X-ray diffraction in a diamond anvil cell at ~2500 K and 125 GPa [*Murakami et al.*, 2004]. This condition is similar to that expected in the D″ layer near the core-mantle boundary (CMB). The post-perovskite structure was independently identified by first principles variable cell shape calculations [*Tsuchiya et al.*, 2004]. Its thermodynamic properties were obtained by means of quasiharmonic free energy calculations and the Clapeyron slope of the post-perovskite transition was shown to be ~7.5 MPa/K [*Tsuchiya et al.*, 2004]. This value is close to that argued to be necessary for a solid-solid transition to account for the D″ discontinuity [*Sidorin et al.*, 1999]. This phase might be the most abundant mineral in the D″ region. However, in order to better understand the relative importance of the post-perovskite phase in this region we need to know its seismic velocities at relevant pressures and temperatures. In particular, seismic anisotropy is observed in various places of the D″ layer [*Kendall and Silver*, 1996, 1998; *Lay et al.*, 1998] and this phenomenon, at least in part, could be attributed to preferred orientation of anisotropic minerals subjected to shear stresses, as expected to occur near the CMB [*Karato*, 1998; *McNamara et al.*, 2002; *Yamazaki and Karato*, 2002]. Lateral heterogeneities are also large in the D″ layer [*Lay et al.*, 1998; *Ishii and Tromp*, 1999] and to better understand its origin it is necessary to understand the elastic properties of post-perovskite at relevant pressures and temperatures. Here we take an important step in this direction and determine various athermal elastic properties of post-perovskite and of its polycrystalline aggregates and compare them with those of the perovskite phase.

2. Calculations and Results

[3] Post-perovskite has the $CaIrO_3$-type structure (space group Cmcm) [*Hyde and Andersson*, 1989]. It consists of SiO_3 layers, formed by columns of edge sharing octahedra connected by the apices, intercalated by eight-fold coordinated magnesium ions. Since its structure is anisotropic, its elastic properties are also expected to be anisotropic. Our first principles calculations use the same technical specifications used in our previous work on this phase [*Tsuchiya et al.*, 2004].

[4] This density functional calculation [*Hohenberg and Kohn*, 1964] used the local density approximation (LDA) [*Ceperley and Alder*, 1980]. We used planewave basis and the same pseudopotentials used before. The planewave kinetic energy cutoff was 70 Ry and the Brillouin zone of the Cmcm primitive lattice was sampled on the $4 \times 4 \times 2$ k-point mesh. The full elastic constant tensor of this orthorhombic structure with nine independent components was calculated using stress-strain relations [*Karki et al.*, 2001]. The magnitude of all applied strains was 0.01. We confirmed that the linear relation was enough ensured for this strain range.

[5] The static elastic constants of post-perovskite are plotted in Figure 1 and shown in Table 1 at two distinct pressures. These values are expected to be overestimated because of the static 0 K nature of this LDA calculation. From the overall behavior of the elastic constants it is clear that the structure is quite anisotropic and that anisotropy is strongly pressure dependent. Two striking features can be immediately noticed in Figure 1: 1) c_{22} is considerably smaller than c_{11} and c_{33} at relevant pressures, and 2) c_{66} is quite large compared with c_{55} and c_{44}. The first feature is typical of layered minerals such as mica, brucite, talc, and so on. It shows this structure is more compressive in the direction perpendicular to the layers (layers parallel to (010)). The second feature is very intriguing. It indicates that a lateral shift of layers ((010) planes) parallel to the edge sharing octahedral columns (along [100]) faces the greatest resistance. This is counterintuitive. In a typical layered structure, lateral shear of layers, along *any* direction, should offer less resistance than the deformation of the layers themselves, here represented by c_{55}. In this structure, the smallest shear elastic constant is c_{44}. It expresses the resistance along [001], i.e., to the lateral shift of layers in the direction perpendicular to the octahedral columns.

0094-8276/04/2004GL020278$05.00

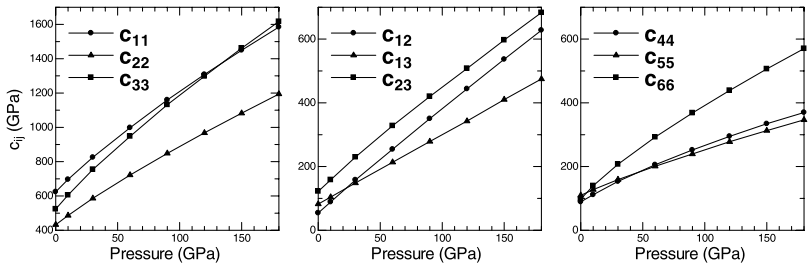

Figure 1. Pressure dependence of the elastic constants of post-perovksite.

[6] The pressure dependence of the isotropic bulk (B) and shear (G) moduli obtained from the Voigt-Ruess-Hill averages [*Hill*, 1963] are shown in Figure 2a along with those of the perovskite structure [*Wentzcovitch et al.*, 2004]. It can be seen that B of both phases are very similar throughout most of the pressure range of the lower mantle. Although post-perovskite's aggregate B, 231 GPa, is smaller than perovskite's, 257 GPa, at $P = 0$ GPa, the larger B' of post-perovskite, 4.3, compensates to produce similar bulk moduli at lower mantle pressures [*Tsuchiya et al.*, 2004]. In contrast, post-perovskite has considerably larger G than perovskite in the pressure range corresponding to the lower part of the lower mantle (7% larger at 120 GPa) even though post-perovskite's G is smaller than perovskite's at 0 GPa. This large G is caused by the large c_{66}. The isotropic averaged compressional (P), shear (S) and bulk (Φ) wave velocities are plotted in Figure 2b. At zero pressure, all velocities are smaller than those of perovskite, while at high pressure, V_P and V_S of post-perovskite are distinctly larger than those of perovskite. V_Φ is quite comparable. The discontinuity in V_S at the static transition pressure of $\sim$100 GPa [*Tsuchiya et al.*, 2004] is 1.5%. This large shear wave velocity of post-perovskite is clearly caused by its large G, despite the larger density of this phase. The post-perovskite transition should be observed preeminently through S wave anomalies.

[7] The single crystal elastic wave velocities shown in Figure 3 were obtained by solving Cristoffel's equation $\det|c_{ijkl}n_jn_l - \rho V^2\,\delta_{ik}| = 0$ [*Musgrave*, 1970]. In this equation $\mathbf{n}$, ρ, V and δ_{ij} are the propagation direction, density, wave velocity and Kronecker delta, respectively. Wave velocities depend on propagation direction and on polarization. For post-perovskite, the difference between V_P and V_S is relatively small compared to the same difference found in perovskite [*Wentzcovitch et al.*, 1998]. This is also caused by the relatively larger G of post-perovskite. Fast and slowest directions change very much with pressure. At 0 GPa V_P is largest and smallest along [100] and [110] respectively. This results from large c_{11} and small c_{66} respectively. At 120 GPa, the slowest direction of the P wave changes to [010], consistent with the small c_{22}. The fastest S waves propagate along [110] and [101], and the slowest along [010] and [001] at 0 GPa. In contrast, at 120 GPa, the fastest directions is along [101] while the slowest are along [100] and [001].

[8] Azimuthal anisotropy for P (A_P) and S (A_S) waves, defined as $A_P = (V_{Pmax} - V_{Pmin})/V_P \times 100$ and $A_S = (V_{Smax} - V_{Smin})/V_S \times 100$, are plotted in Figure 4a. First, they decrease up to about 100 GPa and then remain almost constant. However, at the stable pressure range of post-perovskite, A_P and A_S are much larger than perovskite's [*Wentzcovitch et al.*, 1998] (A's are more than 50% larger). Single crystal anisotropy gives the upper limit on the realistic anisotropy of aggregates. The magnitude of anisotropy due to the lattice preferred orientation (LPO) in aggregates is, in general, much smaller (by a factor of 2 to 3). Another point relevant for extracting information about mantle flow from seismic observations is the anisot-

Table 1. Calculated Elastic Constants (c_{ij}), Bulk (B) and Shear (G) Moduli of Orthorhombic Post-Perovskite $MgSiO_3$[a]

Pressure	c_{11}	c_{22}	c_{33}	c_{44}	c_{55}	c_{66}	c_{12}	c_{13}	c_{23}	B	G
0	624	433	524	89	110	98	54	82	122	231	136
120	1308	968	1298	295	278	439	444	343	507	681	344

[a]Units are given in GPa.

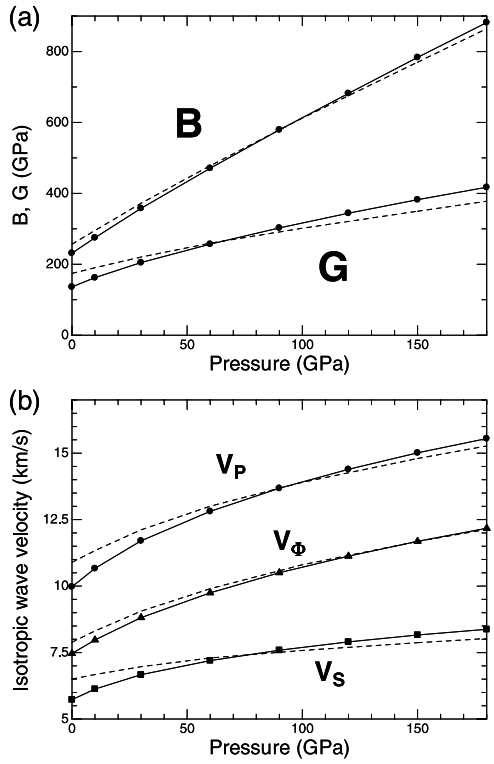

Figure 2. Pressure dependence of the aggregate properties of post-perovskite (solid lines) compared with those of perovskite (dashed lines). (a) Bulk and shear moduli. (b) Compressional, shear, and bulk isotropic wave velocities.

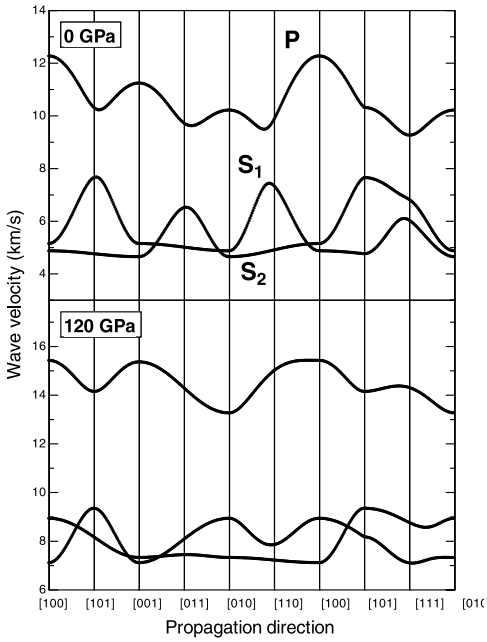

Figure 3. Three single crystal wave velocities (one P and two S waves) of post-perovskite.

ropy produced by transversely isotropic aggregates. This type of aggregate may be caused by LPO's produced under shear flow and can occur at boundary layers. Shear stresses related with changes in flow direction are expected to be particularly large near the CMB. A transversely isotropic medium with a principal vertical axis is characterized by five elastic moduli determined from single-crystal elastic constants [*Love*, 1927; *Montagner and Nataf*, 1986; *Wentzcovitch et al.*, 1998].

[9] *Transverse* anisotropies in V_P and V_S are defined as $A_P^T = (V_{PH} - V_{PV})/V_P \times 100$ and $A_S^T = (V_{SH} - V_{SV})/V_S \times 100$, respectively, where V_{PH} (V_{PV}) is V_P propagating horizontally (vertically), and V_{SH} (V_{SV}) is horizontally (vertically) polarized V_S propagating horizontally. V_S and V_P are the usual isotropic averages. Results are plotted in Figure 4b for aggregates with *a*, *b*, and *c* vertical alignment. As expected in this layered structure A_P^T is the largest for [010] oriented vertically. It can also be seen that A_P^T and A_S^T can be positive or negative depending on the crystalline axes orientation. Contrary to expectations for a layered structure with the slip plane parallel to the layers, A_S^T is small in magnitude and becomes negative at high pressure for [010] aligned vertically. This is because of the counter-intuitively large c_{66} at high pressures. The positively largest A_S^T is achieved with [001] oriented vertically, i.e., layers oriented vertically. Again this is caused by the large values of c_{66} for vertical orientation of layers.

3. Discussion and Conclusions

[10] Although these are static 0 K calculations and high temperature results are necessary before a more reliable analysis of the importance of post-perovskite to D″ can be attempted, these results give the first glimpses on the elastic properties of the newly found phase. First, the stability field of post-perovskite appears to correspond well with that expected in the D″ layer [*Tsuchiya et al.*, 2004]. We see here that, at the transition point, the discontinuity in V_S should be considerably larger than in V_P. This is consistent with reports that the velocity anomaly at the D″ discontinuity is more preeminent in V_S than in V_P [*Wysession et al.*, 1998]. The D″ region is also known to be much more anisotropic than the lower mantle [*Lay et al.*, 1998] and the anisotropy style, i.e., $V_{SH} > V_{SV}$ or vice-versa, varies considerably from place to place [*Pulliam and Sen*, 1998].

[11] Here we show that post-perovskite's azimuthal anisotropy (Figure 4a) is much larger (by 50%) than perovskite's [*Wentzcovitch et al.*, 1998]. This is primarily caused by the small and very large values of c_{22} and c_{66}, respectively. The contrast between perovskite's and post-perovskite's anisotropies could, in principle, produce seismically detectable anisotropy changes across the transition in addition to velocity discontinuities. We also see that the transverse shear anisotropy is very large in magnitude for more than one LPO, in addition to changing sign. Although real fabrics with LPO formed under shear stresses should have some azimuthal anisotropy in the shear plane and should not be completely transversely isotropic, and a better understanding of the rheological properties of post-perovskite is necessary before anything can be stated with more confidence, here we can anticipate from the property of the transversely isotropic medium that LPO's produced by vertical or horizontal flows in D″ could produce quite distinct shear wave splittings. This appears to be consistent

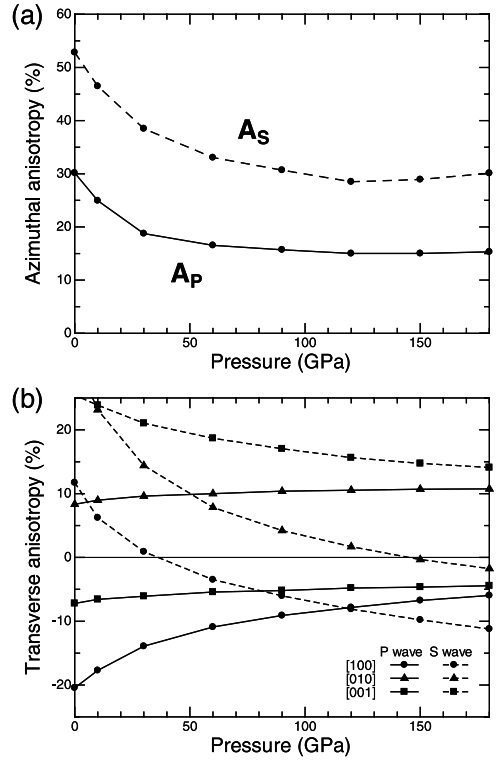

Figure 4. Pressure dependence of the elastic anisotropy (see text) of post-perovskite. (a) Azimuthal anisotropy of P and S waves in single crystal. (b) Azimuthal anisotropy of P waves and polarization anisotropy of S waves in transversely isotropic media with the three possible orientations of the major crystalline axes: *a*, *b*, and *c* oriented vertically.

with the documented lateral variation of anisotropy in D″ [*Lay et al.*, 1998]. The anisotropy style observed underneath the circum-Pacific, i.e., $V_{SH} > V_{SV}$, could be produced by vertical alignments mainly of [001], but perhaps also of [010] (Figure 4b). The former is however much more significant than the latter, contrary to expectations for this layered structure. These elastic properties of post-perovskite indicate that at high pressures the usual notion of a layered structure is not simply applicable to this phase.

[12] In summary, we have shown that $MgSiO_3$-post-perovskite is a highly anisotropic phase. Aggregates of this phase with magnesiowüstite (Mg, Fe)O, the expected secondary abundant phase, also very anisotropic, and another likely candidate for the origin of seismic anisotropy in the D″ [*Yamazaki and Karato*, 2002], could be a source of anisotropy in D″. For more complete understanding of the origin of D″ anisotropy, detailed information on elasticity and plasticity of this two phases aggregate (Post-pv+Mw) at high temperatures, including the effects of Fe, still need to be considered. Only then the importance of chemical stratification and partial melting in generating the observed anisotropy style, $V_{SH} > V_{SV}$ [*Kendall and Silver*, 1996, 1998], can be more fully appreciated.

[13] **Acknowledgments.** We thank S. Karato and G. David Price for helpful suggestions. This research was supported by NSF/EAR 0135533 and 0230319 and by the Minnesota Supercomputing Institute. TT and JT were also supported by the Japan Society for the Promotion of Science (JSPS) for research fellowships.

References

Ceperley, D. M., and B. J. Alder (1980), Ground state of the electron gas by a stochastic method, *Phys. Rev. Lett.*, *45*, 566–569.

Hill, R. (1963), Elastic properties of reinforced solids: Some theoretical principles, *J. Mech. Phys. Solids*, *11*, 357–372.

Hohenberg, P., and W. Kohn (1964), Inhomogeneous electron gas, *Phys. Rev. B.*, *136*, 364–871.

Hyde, B. G., and S. Andersson (1989), *Inorganic Crystal Structures*, 430 pp., Wiley-Interscience, Hoboken, N. J.

Ishii, M., and J. Tromp (1999), Normal-mode and free-air gravity constraints on lateral variations in velocity and density of Earth's mantle, *Science*, *285*, 1231–1236.

Karato, S. (1998), Some remarks on the origin of seismic anisotropy in the D″ layer, *Earth Planets Space*, *50*, 1019–1028.

Karki, B. B., L. Stixrude, and R. M. Wentzcovitch (2001), High-pressure elastic properties of major materials of Earth's mantle from first principles, *Rev. Geophys.*, *39*, 507–534.

Kendall, J.-M., and P. G. Silver (1996), Constraints from seismic anisotropy on the nature of the lowermost mantle, *Nature*, *381*, 409–412.

Kendall, J.-M., and P. G. Silver (1998), Investigating causes of D″ anisotropy, in *The Core-Mantle Boundary Region*, *Geodyn. Ser.*, vol. 28, edited by M. Gurnis et al., pp. 97–118, AGU, Washington, D. C.

Lay, T., Q. Williams, and E. J. Garnero (1998), The core-mantle boundary layer and deep Earth dynamics, *Nature*, *392*, 461–468.

Love, A. E. H. (1927), *A Treatise on the Mathematical Theory of Elasticity*, 4th ed., 643 pp., Cambridge Univ. Press, New York.

McNamara, A. K., P. E. van Keken, and S. Karato (2002), Development of anisotropic structure in the Earth's lower mantle by solid-state convection, *Nature*, *416*, 310–314.

Montagner, J. P., and H. C. Nataf (1986), A simple method for inverting the azimuthal anisotropy of surface waves, *J. Geophys. Res.*, *91*, 511–520.

Murakami, M., K. Hirose, K. Kawamura et al. (2004), Post-perovskite phase transition in $MgSiO_3$, *Science*, *304*, 855–858.

Musgrave, M. J. P. (1970), *Crystal Acoustics*, 288 pp., Holden-Day, Boca Raton, Fla.

Pulliam, J., and M. K. Sen (1998), Seismic anisotropy in the core-mantle transition zone, *Geophys. J. Int.*, *135*, 113–128.

Sidorin, I., M. Gurnis, and D. V. Helmberger (1999), Evidence for a ubiquitous seismic discontinuity at the base of the mantle, *Science*, *286*, 1326–1331.

Tsuchiya, T., J. Tsuchiya, K. Umemoto, and R. M. Wentzcovitch (2004), Phase transition in $MgSiO_3$ perovskite in the Earth's lower mantle, *Earth Planet. Sci. Lett.*, in press.

Wentzcovitch, R. M., B. B. Karki, S. Karato, and C. R. S. Da Silva (1998), High pressure elastic anisotropy of $MgSiO_3$ perovskite and geophysical implications, *Earth Planet. Sci. Lett.*, *164*, 371–378.

Wentzcovitch, R. M., B. B. Karki, M. Cococcioni, and S. de Gironcoli (2004), Thermoelastic properties of $MgSiO_3$ perovskite: Insights on the nature of the Earth's lower mantle, *Phys. Rev. Lett.*, *92*, 018501.

Wysession, M. E., T. Lay, J. Revenaugh et al. (1998), The D″ discontinuity and its implications, in *The Core-Mantle Boundary Region*, *Geodyn. Ser.*, vol. 28, edited by M. Gurnis et al., pp. 273–297, AGU, Washington, D. C.

Yamazaki, D., and S. Karato (2002), Fabric development in (Mg, Fe)O during large strain, shear deformation: Implications for seismic anisotropy in Earth's lower mantle, *Phys. Earth Planet. Inter.*, *131*, 251–267.

T. Tsuchiya, J. Tsuchiya, K. Umemoto, and R. M. Wentzcovitch, Department of Chemical Engineering and Materials Science, Supercomputing Institute, University of Minnesota, 421 Washington Avenue SE, Minneapolis, MN 55455, USA. (takut@cems.umn.edu)